# Effects of process conditions on the chemistry of an Ar/C2H2 dust-forming plasma

Igor Denysenko, Erik von Wahl, Safa Labidi, Maxime Mikikian, Holger Kersten, Titaïna Gibert

HAL Id: hal-02092526
https://hal.science/hal-02092526

Submitted on 18 Apr 2020

# Effects of Process Conditions on the Chemistry of an Ar/C₂H₂ Dust-Forming Plasma

Igor B. Denysenko*, Erik von Wahl, Safa Labidi, Maxime Mikikian, Holger Kersten, Titaïna Gibert

_____

Prof. I. B. Denysenko

School of Physics and Technology, V. N. Karazin Kharkiv National University,

4 Svobody sq. 61022, Kharkiv, Ukraine

E-mail: idenysenko@yahoo.com

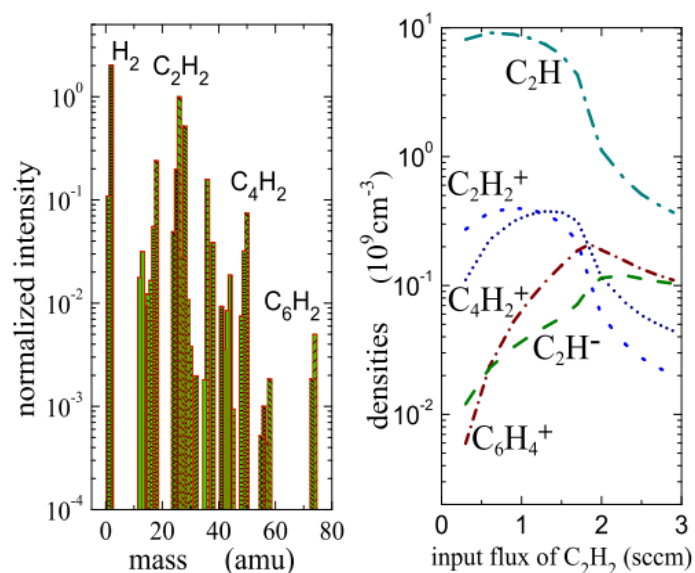E. von Wahl, S. Labidi, Dr. M. Mikikian, Dr. T. Gibert

GREMI, UMR7344 CNRS/Université d'Orléans, Orléans, F-45067, France

E. von Wahl, Prof. H. Kersten

Institut für Experimentelle und Angewandte Physik, Christian-Albrechts-Universität zu Kiel,

Kiel, 24098, Germany

A volume-averaged model and numerical simulations are used to clarify the effects of process conditions on the plasma chemistry and species initiating the formation of nanoparticles in an Ar/$C_2H_2$ plasma. It is shown that Ar/$C_2H_2$ plasmas with low electron density, moderate input flux of acetylene and an electron energy distribution function (EEDF) close to the Druyvesteyn EEDF are the most suitable for the production of carbonaceous nanoparticles. These results are verified by a direct comparison with experimental data and enable to formulate recommendations for future experiments with a controlled growth of nanoparticles in chemically-active plasmas.

# 1.    Introduction

Plasmas with nano- and micrometre-sized particles (dust particles) are useful for various applications[1−5] and are also of great fundamental interest.[6−10] The dust particles can either be injected into laboratory plasmas from outside or can grow inside due to different chemical reactions. For example, formation of carbonaceous dust particles takes place in reactive plasmas operating in mixtures of different gases with methane, acetylene or ethylene.[11−13]

In the past two decades, plasmas used for the formation of carbonaceous dust particles have been intensively investigated both by experimental measurements[11−21] and numerically.[21−28] The experiments have shown that dust particle growth strongly depends on the concentrations of $C_2H^-$ ions, which are supposed to act as a main species for the initiation of dust formation,[11] and $C_2H$ neutral radicals.[16] The experiments also revealed that the formation of dust particles in $Ar/C_2H_2$ plasmas is accompanied by a decrease of the electron and acetylene densities and by an increase of the electron temperature and the density of metastable argon atoms.[16-20] Numerical simulations of the nucleation of nanoparticles in $C_2H_2$ and $Ar/C_2H_2$ plasmas showed that positive and negative ions, as well as hydrocarbon radicals may take part in the initial stage of particle formation.[22−27]

The experiments on nanoparticle growth have also revealed that the growth is possible only at certain process conditions (pressure, discharge power, input gas fluxes, etc.). Varying the conditions can affect the internal plasma parameters as the electron, ion and neutral densities and the electron energy distribution function. To initiate the nanoparticle formation, certain internal conditions are required. In particular the densities of species taking part in the nucleation of nanoparticles should be above threshold values.[16]

However, in most numerical studies on plasmas used for the formation of carbonaceous nanoparticles, it was not analysed how different process conditions affect the species which may initiate nanoparticle growth (negative and positive hydrocarbon ions and hydrocarbon radicals), while in most experiments, the process conditions suitable for

nanoparticle formation have been chosen empirically. To control the dust particle growth, a fundamental understanding of the involved chemical processes and the role of process conditions on species initiating the nanoparticle growth have to be revealed.

In this paper, we analyse how the properties of an Ar/$C_2H_2$ plasma (the ion, electron and neutral particle densities, the electron temperature and the dust charge) depend on several key process conditions: discharge power, acetylene input flux, shape of the electron energy distribution function and nanoparticle density. Moreover, processes responsible for the production and loss of different ions and neutrals in the discharge are analyzed, in order to identify the most important ones. The numerical study is carried out for process conditions similar to our experiments on nanoparticle growth[21,29] using a global (volume-averaged) model. The 0D model approach has shown to be effective for the analysis of chemically-active gas dischargers at low pressures.[30−32] Finally, we discuss, which process conditions are the most suitable for nanoparticle genesis.

## 2. The Model

The model considers an Ar/$C_2H_2$ plasma of $R = 22$ cm radius and $L = 32.4$ cm height sustained in a cylindrical stainless steel chamber as in the experiment of interest.[21,29] To analyze the plasma properties, a volume-averaged model is used assuming that the plasma consists of electrons with density $n_e$, nine positive ions ($C_2H_2^+$, $Ar^+$, $ArH^+$, $H_2^+$, $H^+$, $C_4H_3^+$, $C_4H_2^+$, $C_6H_4^+$ and $C_2H_3^+$), four nonradical neutrals (Ar, $C_2H_2$, $H_2$ and $C_4H_2$), two radicals ($C_2H$ and H), metastable argon atoms ($Ar_m$) with density $n_m$, argon atoms in the resonance 4s states ($^3P_1$ and $^1P_1$) ($Ar_r$) with density $n_r$ as well as argon atoms in 4p states (Ar(4p)) with density $n_{4p}$ and negatively charged dust particles with density $n_d$, radius $a_d$ and charge $Z_d$ (in units of electron charge $e$). In the 0D model, densities $n_m$, $n_r$ and $n_{4p}$ represent composite levels of: $^3P_0$ and $^3P_2$ (metastable), $^3P_1$ and $^1P_1$ (resonance) and 4p states, respectively. The model takes into account the most important neutral species and positive ions evidenced in

our experiments on nanoparticle growth in an Ar/C₂H₂ plasma (**Figure 1**). The details of the experiments can be found elsewhere[21,29]
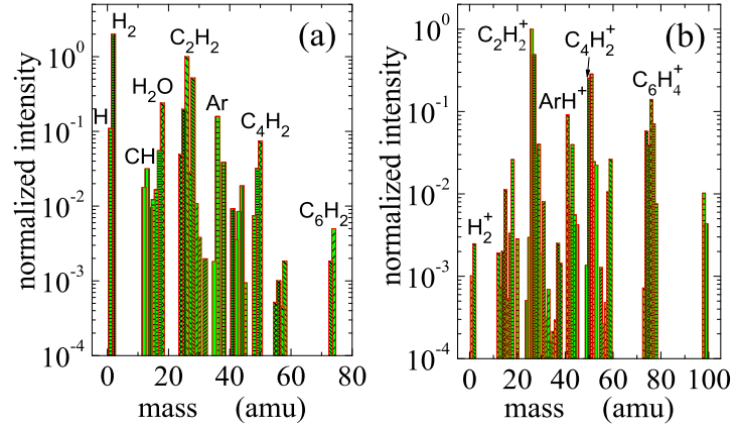


*Figure 1*. Mass spectra for neutral species (*a*) and positive ions (*b*) measured in our experiments on growth of nanoparticles for the growth time when the dust radius is nearly 25 nm. The Ar/C₂H₂ plasma discharge was driven at 13.56 MHz and a radio-frequency power of 9 W. The plasma height $L$ and radius $R$ were nearly 32.4 cm and 22 cm, respectively. Acetylene with the flux $Q_{C2H2}$=1.5 sccm and argon with the flux $Q_{Ar}$=11 sccm were used as a reactive precursor and a background gas, respectively. The process gas pressure in the reactor was about 4.2 Pa.

The dominant neutral species are argon atoms with their density $n_{Ar} \approx P/(k_B T_g) \approx$ $1.01 \times 10^{15}$ cm⁻³, with $P = 4.2$ Pa is the pressure of argon gas, $k_B$ is the Boltzmann constant and $T_g$ is the gas temperature considered to be 300 K. Note that in our mass spectra measurements[21] we were not able to measure intensities of argon ions and neutrals at mass 40 amu simultaneously with other species because the intensity was much above saturation and the instrument would shut down. We assume that the energy distribution for ions is Maxwellian, and that ions and dust particles are at gas temperature. We also assume that the plasma contains negative ions C₂H⁻ with density $n^-$ although not measured in our experiment

due to mass spectrometer limitations and complexity in extracting negative ions from the positive plasma glow. At large ratio of the argon atom density to that of acetylene molecules, the anions $C_2H^-$ are the dominant negative ions.[26,27]

In the model, the electron energy distribution function (EEDF) is allowed to vary according to the general distribution function given by[31,33]

$$F(\varepsilon) = A_1 \varepsilon^{1/2} \exp(-A_2 \varepsilon^x), \tag{1}$$

where $\varepsilon$ is the electron energy and $x$ is a number with $x = 1$ or $x = 2$ for Maxwellian or Druyvesteyn electron energy distributions, respectively. The coefficients $A_1$ and $A_2$ are functions of the number $x$ and average electron energy[31,33] $\langle \varepsilon \rangle = \int_0^\infty \varepsilon F(\varepsilon) d\varepsilon = \frac{3}{2} e T_{eff}$, where $T_{eff}$ is the effective electron temperature. The EEDF has the following normalization $\int_0^\infty F(\varepsilon) d\varepsilon = 1$.

The plasma is assumed to be quasineutral, or

$$\sum_\alpha n_\alpha^+ = n_e + n^- + |Z_d| n_d, \tag{2}$$

where $n_\alpha^+$ is the density of the α-th positive ion species.

The volume-averaged model consists of the particle balance equations for ions and neutrals, the power balance equation and the equation for the dust charge. In this study, we consider various processes for the generation and loss of the discharge species, including collisional processes in the bulk plasma, processes on the plasma walls and dust particles, as well as pumping gas in and out of the chamber. In the power balance, we accounted for the power loss due to electron-neutral collisions and the losses due to charged particle fluxes to the walls and dust particles. The electron-molecule (atom) and ion-molecule (atom) processes, the reactions for neutral-neutral collisions, the details concerning the model equations, as well

as the numerical method of their solution are described in detail in the Supporting information and can also be found in ref.[21]


## 3. Results of Calculations and Discussion

Using the volume-averaged model, we have analyzed how the $Ar/C_2H_2$ plasma properties depend on different process conditions (absorbed power, EEDF, input flux of $C_2H_2$ and nanoparticle density). The study has been carried out for the conditions similar to our experiments on nanoparticle growth.[21]  Main processes responsible for the generation and loss of different ions and neutral species have also been analysed and are presented in the Supporting information. In most cases studied here, the EEDF is considered to be Druyvesteyn-like as it is typical for radio-frequency laboratory plasmas at $n_e < 10^{11}$ cm$^{-3}$ and $Pd > 0.2$ Torr×cm,[34] where $d \approx L/2$ is the dimension of reactor in cm, i. e., for the conditions of our experiments.[21,29] As grown nanoparticles may affect the EEDF[35,36], the study of its variation on the plasma properties is also of particular interest.


## 3.1.  Effects of Variation in Discharge Power on the Densities of Ions and Neutral Species

First, we analyze how the properties of an $Ar/C_2H_2$ plasma depend on the absorbed power $P_{abs}$. An increase of $P_{abs}$ leads to an elevation in the electron density (**Figure 2a**), while the electron temperature only slightly depends on a power variation and remains at $T_{eff} \approx 3$ eV.

The increase of $n_e$ at increasing $P_{abs}$ is accompanied by an increase of the densities of excited argon atoms Ar* (Figure 2a) and the densities of Ar$^+$, $C_2H_2^+$, $C_4H_3^+$, $C_4H_2^+$, ArH$^+$, H$^+$, $H_2^+$, $C_6H_4^+$ (only for $P_{abs} < 7$ W) and $C_2H_3^+$ (only for $P_{abs} < 10$ W) (Figure 2b,c) because of an increasing number of electron-neutral collisions involving argon atoms and nonradical molecules. The $C_2H_3^+$ and $C_6H_4^+$ densities decrease for large $P_{abs}$ (Figure 2b,c) due to the disappearance of the nonradical molecules $C_2H_2$ and $H_2$ ($C_2H_2^+ + H_2 \rightarrow C_2H_3^+ + H$, $C_4H_2^+ + C_2H_2 \rightarrow C_6H_4^+$) (Figure 2d).
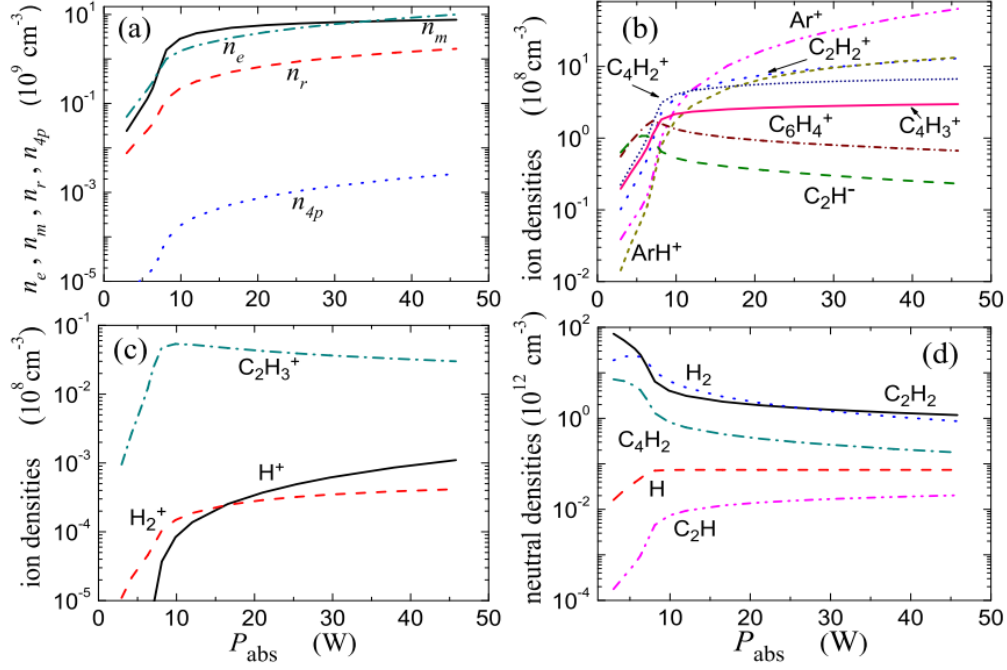
*Figure 2.* The densities of electrons and argon atoms in excited states (*a*), ions [(*b*) and (*c*)] and neutral species (*d*) as functions of the absorbed power. The dependencies are obtained for $Q_{C2H2}$=1.5 sccm, $Q_{Ar}$=11 sccm, $x = 2$, $L$= 32.4 cm, $R = 22$ cm and $n_d = 0$.

Indeed, with the increase of the discharge power, densities of $C_2H_2$, $C_4H_2$ and $H_2$ ($H_2$ only for $P_{abs} > 5.6$ W) decrease as they are mainly lost in collisions with electrons, positive ions, $C_2H$ radicals and argon atoms in different excited states (see the Supporting information). The density of $H_2$ slightly increases at small absorbed powers ($P_{abs} < 5.6$ W) due to an increase of the H density as $H_2$ is mainly produced by collisions of H with the walls.

The H atoms are mainly generated by electron-impact dissociation and ionization of $H_2$, in collisions of Ar* with $C_2H_2$, $C_4H_2$ and $H_2$ and in collisions of $C_2H$ with $C_2H_2$ and $H_2$ (see the Supporting information). Due to an enhancement of these production processes, the H density becomes larger with increasing $P_{abs}$ for $P_{abs} < 10$ W. For larger absorbed powers, production and loss processes counterbalance, leading to a nearly constant H concentration. The density of $C_2H$ radicals grows with increasing $P_{abs}$ because of the also growing Ar*

concentration ($C_2H$ is mainly produced in collisions between $C_2H_2$ molecules with electrons and Ar* atoms) and because of the decrease in $C_2H_2$ density ($C_2H$ is mainly lost in collisions with acetylene molecules).

Finally, it can be seen, that the $C_2H^-$ concentration is growing with $P_{abs}$ for low absorbed powers ($P_{abs} < 5.6$ W) but then descending for high $P_{abs}$. This originates from the interplay of an enhancement of the $C_2H^-$ production in collisions between electrons with $C_2H_2$ on one hand and an enhancement of anion losses in collisions with positive ions and hydrogen atoms (see the Supporting information) on the other hand.

For the experimental conditions ($n_e = 1.28 \times 10^9$ cm$^{-3}$, $P_{abs} = 9$ W), the simulation shows that the dominant neutrals in the plasma are Ar, $C_2H_2$ and $H_2$, while the dominant ions are $Ar^+$, $C_2H_2^+$, $C_4H_2^+$, $C_4H_3^+$, $C_6H_4^+$ and $ArH^+$. The densities of $H_2^+$ and $H^+$ are essentially smaller than those of other ions. This agrees well with our measurements of mass spectra for neutral species and positive ions for plasmas largely affected (Figure 1) and little affected by the nanoparticle presence.[21] Therefore, the model description of the reactive chemistry can generally be regarded as valid with the ability to reproduce experimental trends qualitatively.

To summarize, under our experimental conditions (i.e. $P_{abs} \sim 9$ W), we find a relatively large amount of all the species taking part in the initial stage of nanoparticle formation:[16,23,25] $C_2H^-$ ($\sim 10^8$ cm$^{-3}$ as in ref.[25]), $C_2H$ ($\sim 6.0 \times 10^9$ cm$^{-3}$) and most of the reactive positive ions (for example, the density of $C_6H_4^+$ is $1.4 \times 10^8$ cm$^{-3}$). Therefore, our power regime may be favorable for nanoparticle nucleation.

## 3.2. Effects of Variation in Shape of the Electron Energy Distribution Function

In the following, we will analyse how the plasma properties depend on the EEDF shape that can for example be influenced by the choice of plasma source. For that, we will vary the parameter $x$ in Equation (1), while other process parameters remain fixed.

In **Figure 3a,b**, the effective electron temperature and the densities of electrons and metastable argon atoms as functions of $x$ are shown. One can see that $n_m$ and $T_{eff}$ are increasing with $x$, while the electron density drops. The correlation between $T_{eff}$ and $x$ comes from a more convex electron energy probability function (EEPF), $F(\varepsilon)/\varepsilon^{1/2}$, and, as a result, the number of electrons in the energy range $3\text{ eV} < \varepsilon < 17\text{ eV}$ grows with respect to their total number (Figure 3c). It is also accompanied by an increasing $n_m$ (Figure 3a) and by an enhancement of the power loss per electron in various electron-neutral inelastic collisions. Because of the power loss enhancement, the electron density decreases (Figure 3b). Note that for a pure argon plasma, in ref.[33] it was also found that $T_{eff}$ grows and $n_e$ becomes smaller with an increase of $x$.
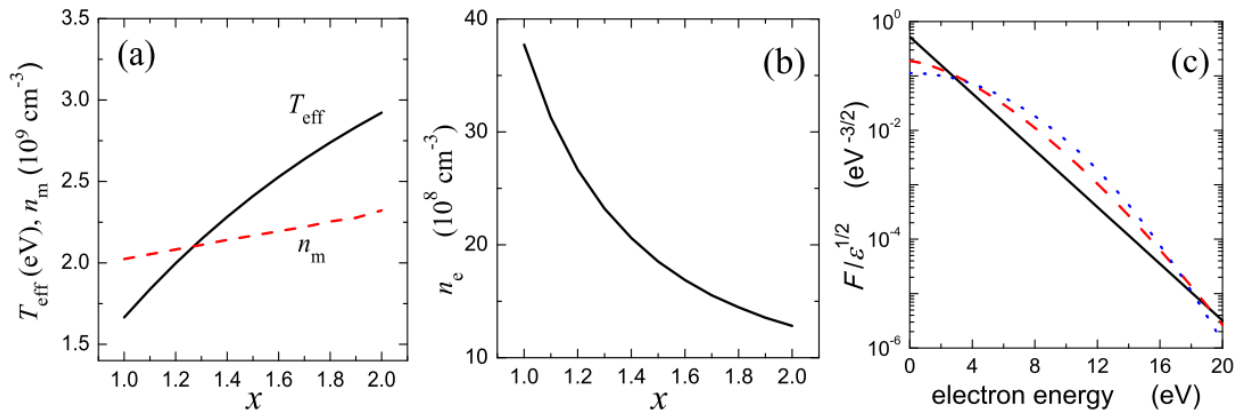


*Figure 3.* $n_m$ (a), $T_{eff}$ (a), $n_e$ (b) as functions of $x$. c) The EEPFs for $x = 1$ (solid curve), $x = 1.5$ (dashed curve) and $x = 2$ (dotted curve). Here, $T_{eff} = 1.67$ eV, 2.41 eV and 2.92 eV for $x = 1.0$, 1.5 and 2.0, respectively. The dependencies are calculated for $P_{abs} = 9$ W and the other parameters are the same as in Figure 2.

As a result of the $n_e$ reduction, the density of acetylene molecules is slightly enhanced for greater values of $x$ (**Figure 4a**). This is accompanied by greater $C_4H_2$ and $H_2$ concentrations. Additionally, increasing the $C_2H_2$ density and $n_m$ makes the reaction $Ar_m + C_2H_2 \rightarrow C_2H + Ar + H$ more probable, so that the $C_2H$ density slightly grows with $x$. The amount of atomic hydrogen also grows with $x$. In our opinion, this is mainly due to an

enhancement of the H production in collisions of $C_2H$ with $C_2H_2$ and of $Ar^*$ with $C_2H_2$, $C_4H_2$ and $H_2$ (see the Supporting information).

The densities of positive ions, however, drop with increasing $x$ (Figure 4b) because of greater losses in collisions with neutral species, whose densities become larger, and because of a lower production in electron-neutral collisions (because of the $n_e$ decrease). On the contrary, the density of $C_2H^-$ slightly grows with $x$ for $x \leq 1.3$ but then also slightly decreases at larger $x$. This dependence on $x$, in our opinion, is mainly due to a combination of losses in collisions with positive ions and H. At small $x$, the former process is dominant while at large $x$, the latter one takes over. Therefore, the maximum density of anions is found for moderate $x$ values.
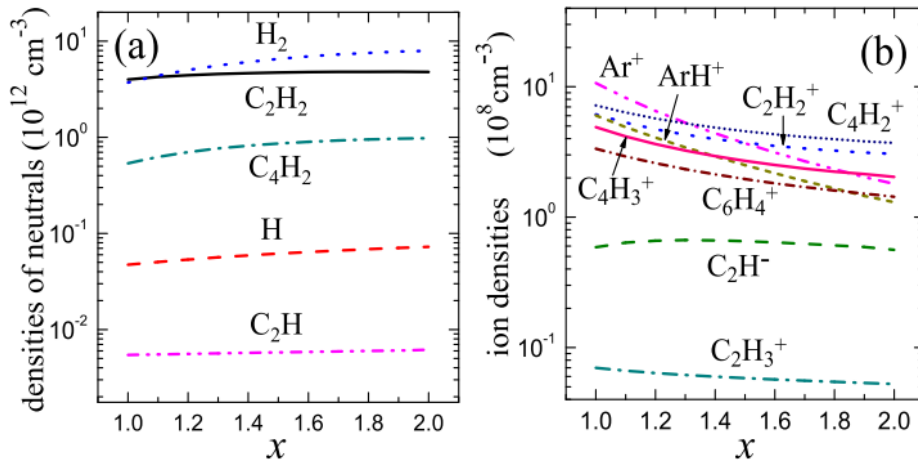


*Figure 4.* The densities of neutral species (a) and ions (b) as functions of $x$ for the same conditions as in Figure 3.

## 3.3   Effects of Variation in Acetylene Input Flux

Next, we analyse how a variation of the $C_2H_2$ input flux affects the plasma properties and the chemical composition. An increase of $Q_{C2H2}$ naturally leads to an elevation in the $C_2H_2$, $H_2$ and $C_4H_2$ densities (**Figure 5a**). Thus, the power losses by inelastic collisions of electrons with these molecules increase. As a result, for a fixed absorbed power (here, $P_{abs} = 9$ W) a

higher $Q_{C2H2}$ causes a lower electron density (Figure 5c). Due to the small amount of electrons, the densities of excited argon atoms, including metastables, then decrease too (Figure 5c). With increasing $Q_{C2H2}$, the effective temperature slightly decreases from 2.96 eV up to 2.9 eV in the range 0.3 sccm $\leq Q_{C2H2} \leq$ 1.7 sccm and slightly increases at higher $Q_{C2H2}$ (for example, $T_{eff}$ = 3.12 eV for $Q_{C2H2}$ = 2.9 sccm).
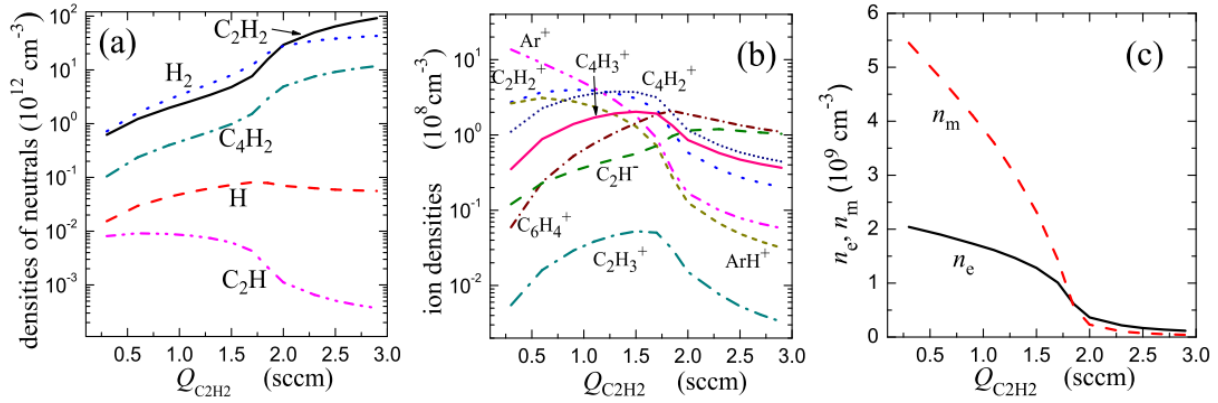


*Figure 5.* The densities of neutral species (a), ions (b), electrons (c) and argon atoms in the metastable states (c) as functions of the acetylene input flux. The dependencies are obtained for $P_{abs}$ = 9W and the other external parameters are the same as in Figure 2.

Since the production and loss of ions and radicals in the Ar/$C_2H_2$ plasma depend on the electrons, Ar*, $H_2$, $C_2H_2$ and $C_4H_2$ densities, their $Q_{C2H2}$ dependencies indirectly determine the ones for ions and radicals (Figure 5a,b). In particular, due to the reduction of $n_e$ and $n_m$ for higher $Q_{C2H2}$, the production and density of Ar$^+$ also decrease, in turn leading to the decrease in the ArH$^+$ density. At small $Q_{C2H2}$, the densities of positive hydrocarbon ions grow with $Q_{C2H2}$ because of the $C_2H_2$ and $C_4H_2$ density increase (the ions are produced from these molecules). At large $Q_{C2H2}$, however, the hydrocarbon cation densities drop due to an enhancement of their losses in collisions with molecules, whose densities are growing at the same time, and due to a decrease of their production in collisions with electrons and Ar* (their densities are reduced).

For $Q_{C2H2} < 2.3$ sccm the density of $C_2H^-$ anions grows with $Q_{C2H2}$ due to the likewise growing $C_2H_2$ density and due to the reduction of the total density of positive ions (the anions are produced in collisions of electrons with acetylene molecules, while their loss is due to the collisions with positive ions and hydrogen atoms). At $Q_{C2H2} > 2.3$ sccm, the $C_2H^-$ concentration slightly decreases with a further $Q_{C2H2}$ increase because of the reduced electron density. Since the production of the $C_2H$ radical mainly takes place in collisions of electrons and excited argon atoms with acetylene molecules, the decrease in electron and excited atom densities at increasing $Q_{C2H2}$ is accompanied by a reduction of the $C_2H$ density.

### 3.4. Effects of Variation in Dust Density

The formation of nanoparticles in the plasma may essentially affect the discharge properties due to the collection of electrons, ions and radicals by the dust particles. As a result, the electron density decreases and $T_{eff}$ grows when $n_d$ becomes larger (**Figure 6a,b**). In turn, due to the increase of $T_{eff}$, the density of metastable argon atoms also grows as long as the dust amount stays below $n_d < 3 \times 10^7$ cm$^{-3}$ (Figure 6b). At $n_d > 3 \times 10^7$ cm$^{-3}$, $n_m$ drops again because of a decrease in $n_e$. Furthermore, the increase in $T_{eff}$ also enhances the production of $Ar^+$ in electron-atom collisions (Figure 6c). This is accompanied by an enhancement of the $ArH^+$ production in collisions of $Ar^+$ with $H_2$, and thus, leads to an increase in the $ArH^+$ density and to a decrease in the $H_2$ density (Figure 6d). As $C_2H_2$ is mainly lost in collisions with Ar* atoms, the $C_2H_2$ density evolves inversely to $n_m$. In turn, the $C_4H_2$ production is related to the $C_2H_2$ density,[17] and, as a result, the $n_d$ - dependencies of both molecules are similar.
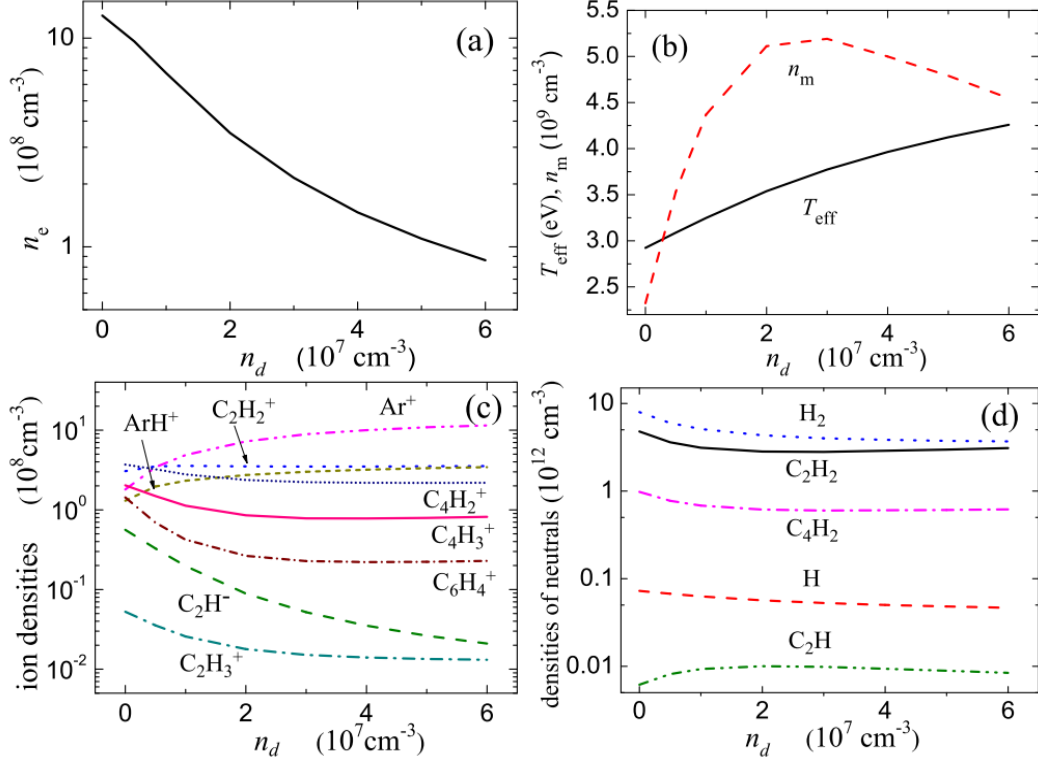
*Figure 6*. The density of electrons (a), $n_m$ and $T_{eff}$ (b), the ion densities (c) and the densities of neutral species (d) as functions of the dust density. The dependencies are calculated for $a_d = 25$ nm, $Q_{C2H2} = 1.5$ sccm and the other parameters as in Figure 5.

At large dust densities, the deposition on dust particles is the dominant loss process for most hydrocarbon ions (see the Supporting information) and their densities are smaller than in the $n_d = 0$ case. The concentration of negative ions $C_2H^-$ becomes smaller for larger $n_d$ mainly due to a reduction of the anion generation through electron attachment to $C_2H_2$ (since $n_e$ decreases), as well as due to an enhancement of the negative ion loss in collisions with $Ar^+$ ions.

Note that the $n_d$-dependencies for $T_{eff}$ and the densities of neutrals, ions and metastable atoms (Figure 6) are similar to the corresponding $a_d$-dependencies presented in ref.,[21] where the $a_d$-dependencies for neutral species were found to be in a good qualitative agreement with experimental results.

In our experiments on growth of nanoparticles,[21,29] the mass spectra for neutral species and positive ions were measured at different times during the growth cycle of nanoparticles: (i) when the nanoparticles are sufficiently small to not modify plasma properties and (ii) when the nanoparticle size and number density are large enough to strongly disturb the plasma. The dust radius for the case (ii) was found to be about 25 nm,[29] and the corresponding mass spectra are presented in Figure 1. The electrode self-bias voltage in the case (i) was larger (more than − 200 V) than that in the case (ii) (about − 100 V).[29] It was found that in the case (ii), the mass peaks of $H_2$ and H are respectively, 9 % and 5 % larger than the mass peaks in the case (i) whereas the mass peaks of $C_2H_2$, $C_2H$ and $C_4H_2$ are, respectively, 15%, 14% and 9% smaller.

It was also found that the mass peaks of most ions in the plasma with large nanoparticle size and number density are smaller than the peaks for the case when dust particles do not affect much on plasma properties. In particular, the mass peaks of $C_2H_2^+$, $C_2H_3^+$, $ArH^+$, $C_4H_2^+$ and $C_4H_3^+$ in the case (ii) are, respectively, 25%, 20%, 55%, 26% and 19% smaller than the mass peaks in the case (i). However, the peaks at mass numbers 20 (for $Ar^{++}$), 38 (for $Ar^+$) and 76 (for $C_6H_4^+$) are, respectively, 55%, 21% and 33% larger in the case of large dust density.

Thus, the results of our calculations agree well with the experimental data. In particular, the calculated densities of $C_2H_2$, $C_4H_2$, $C_2H_3^+$, $C_4H_2^+$ and $C_4H_3^+$ are smaller and the density of $Ar^+$ is larger in a plasma with large dust density and size than in the dust-free case (Figure 6).

However, there is a discrepancy between the results of our calculations and the experimental data for some species ($ArH^+$, $C_2H_2^+$, $H_2$, H, $C_2H$ and $C_6H_4^+$). This difference is due to different reactions in the mass-spectrometer (for example, the measured mass peak of $C_2H$ originates mainly from the dissociation of $C_2H_2$ in the ion source of the mass spectrometer[37]). It is also because the mass spectra measurements were conducted in one

point of the plasma volume (at a height of 10 cm and a radial distance of 7 cm from the center of the powered electrode), and, therefore, the measured compositions of ions and neutrals may be different from those averaged on the plasma volume. The difference between the numerical and experimental results may also be due to various simplifications used in the model. In particular, our global model assumes that the dust particles are nearly uniformly distributed in the plasma volume, while numerous experiments show that the spatial distribution of dust particles is usually essentially inhomogeneous in dusty plasmas.[7,38] Therefore, the model here is applicable only for a qualitative analysis of $Ar/C_2H_2$ dusty plasmas and should be improved by inclusion of the effects of spatial nonuniformity of dust density.

Note also that in our model it is assumed that the ion temperature equals the gas temperature. Meantime, because of ion acceleration in inhomogeneous plasma regions, the spatially-averaged ion temperature is slightly larger than the gas temperature. Therefore, we checked how a deviation of the ion temperature from $T_g$ affects the results of our calculations. We carried out our calculations for the dusty plasma case at $T_i = 350$ K and $T_i = 450$ K. The calculations were carried out assuming that $T_g = 300$ K, $n_d = 10^7$ cm$^{-3}$ and the other external conditions are the same as in Figure 6. Indeed, it was found that a variation of the ion temperature slightly affects some plasma properties. In particular, the densities of $C_2H_2$ and $H_2$ and $n_e$ at $T_i = 300$ K differ by less than 1% from these densities at $T_i = 350$ K and $T_i = 450$ K. The electron temperature is also nearly independent on $T_i$ (~3.25 eV) for the ion temperatures considered here. With increasing $T_i$, the dust charge $Z_d$ slightly increases ($Z_d = -81$, $-83$ and $-88e$ for $T_i = 300$, 350 and 450 K, respectively) because of decreasing the rate describing collection of positive ions of sort $\alpha$ by dust particles ($K_d^\alpha \approx a_d^2 \left(8\pi T_i/m_i\right)^{1/2} \left(1 + \xi\tau + H\xi^2\tau^2\lambda_s n_n \sigma_{in}\right)$).[39] Here, $\tau = T_{\text{eff}}/T_i \gg 1$, $m_i$ is the ion mass, $n_n$ is the total neutral density, $\sigma_{in} \approx 10^{-14}$ cm$^2$ is the cross-section for ion neutral collisions and $\xi = |Z_d|e^2/a_d T_{\text{eff}}$. The function $H$ satisfies $H \sim 0.1$ for $0.1 \leq \beta \leq 10$, $H \sim \beta$ for $\beta \ll 1$,

and $H \sim \beta^{-2}(\ln\beta)^3$ for $\beta \gg 1$,[39] where $\beta = |Z_d|e^2/\lambda_s T_i$, and $\lambda_s$ is the screening length, which is of the same order as the Debye length.[1] Because of decreasing the rate for collection of positive ions by dust particles, the densities of positive ions are slightly increasing with an increase of $T_i$ (for $T_i$ = 300, 350 and 450 K, $n_{Ar}^+$ = 4.88×10$^8$, 4.95×10$^8$ and 5.04 ×10$^8$ cm$^{-3}$, $n_{C2H2}^+$ = 3.57×10$^8$, 3.59×10$^8$ and 3.67 ×10$^8$ cm$^{-3}$, respectively), while the density of negative ions is nearly independent on $T_i$ ($n^- \sim$ 1.97 ×10$^7$ cm$^{-3}$).

## 4. Summary and Recommendations for Developing Future Experiments

Our numerical study of an Ar/C$_2$H$_2$ plasma under typical conditions for the growth of nanoparticles has demonstrated that the densities of species taking part in the nanoparticle nucleation (negative and positive hydrocarbon ions and hydrocarbon radicals) depend on various process parameters. Accordingly, for the designing of future experiments on the controlled growth of nanoparticles in Ar/C$_2$H$_2$ plasmas, we recommend to take into account the following factors and effects:

1) Through changing the electron density, for example by varying the input power, one can enhance or suppress the production of the species taking part in the nanoparticle formation. The amount of negative ions, which are in particular assumed to be main species for the initiation of nanoparticle formation,[16] goes up with $n_e$ ($P_{abs}$) for small electron densities (here, $n_e$ < 2×10$^8$ cm$^{-3}$ at $P_{abs}$ < 5.6 W) but goes down for $n_e$ > 2×10$^8$ cm$^{-3}$. An increase in the electron density is accompanied by a density reduction of the C$_2$H$_2$ and C$_4$H$_2$ molecules, which participate in the formation of large molecules and anions (for example, in the reaction C$_{2n}$H$^-$ + C$_2$H$_2$ → C$_{2n+2}$H$^-$ + H$_2$,[23,27] where n is a natural number). Since both, the anion and hydrocarbon molecule densities, are small at large $n_e$ ($P_{abs}$), an Ar/C$_2$H$_2$ plasma with low or moderate electron density is, in our opinion, more suitable for nanoparticle production than one with large $n_e$. It may be a

reason why most of the nanoparticle growth experiments in Ar/$C_2H_2$ are performed at relatively low power. [16,17,29]

2) The densities of plasma species also depend on the shape of the electron energy distribution function. The densities of $C_2H^-$, $C_2H_2$ and $C_4H_2$ are larger in a plasma where electrons have the Druyvesteyn energy distribution than in the case of a Maxwellian EEDF because the effective electron temperature is larger and the electron density is smaller in the former case. Therefore, in our opinion, plasmas where the EEDF is close to the Druyvesteyn distribution (for example, in capacitively coupled plasmas with $f = 13.56$ MHz, $n_e < 10^{11}$ cm$^{-3}$ and $Pd > 0.2$ Torr×cm[34]) are more suitable for the production of nanoparticles.

3) Moreover, the Ar/$C_2H_2$ plasma properties depend on the ratio of the acetylene input flux to that of argon. The results of our study reveal that for nanoparticle growth the input flux of $Q_{C2H2}$ should be moderate. For example, in our experiment, the optimal flux of $C_2H_2$ is empirically found to be around 1.5 sccm. At smaller input fluxes, the formation of nanoparticles is less probable because of small densities of $C_2H^-$ and $C_2H_2$. At large $Q_{C2H2}$, however, the formation of particles may lack enough $C_2H$ radicals and positive hydrocarbon ions.

4) Dust particles can essentially affect the plasma properties (Figure 6). The density of negative ions goes down with an increase of $n_d$ due to an enhancement of the anion losses in collisions with more abundant argon ions and due to a reduced anion production through the attachment of electrons to acetylene molecules. The latter is caused by the decrease in the electron density (Figure 6a). Therefore, the growth of new nanoparticles in a plasma already containing large dust charge density $n_d|Z_d|$ should be supressed or be less intensive than in a dust-free plasma. This may be a reason why nucleation is limited to the beginning of a dust growth cycle, and hence, why the nanoparticles exhibit a monodisperse size distribution.[29] It also confirms why

new generations of nanoparticles appear in dust-free regions like the void or once the former generation has been evacuated from the plasma under the action of detrapping forces.[16,40,41]

## 5.    Conclusion

Our numerical results have shown how the properties of an $Ar/C_2H_2$ plasma depend on the input power, the acetylene input flux, the shape of the electron energy distribution function and the density of nanoparticles. In particular, it has been analyzed how the process parameters affect the densities of ions and neutral species in the plasma, including the densities of species taking part in the nanoparticle nucleation. Using these analyses, recommendations on the controlled growth of nanoparticles in $Ar/C_2H_2$ plasmas have been formulated. It has been concluded that $Ar/C_2H_2$ plasmas at low discharge power, moderate input flux of acetylene and with the electron energy distribution close to the Druyvesteyn EEDF are preferable for the production of carbonaceous nanoparticles. The obtained results are relevant to many applications involving chemically-active plasmas containing impurities, especially gas discharge plasmas used for the synthesis of novel nanomaterials.

Supporting Information is available from the Wiley Online Library or from the author.

[1] *Dusty Plasmas: Physics, Chemistry, and Technological Impacts in Plasma Processing*, A. Bouchoule, Eds., Wiley, New York **1999**.

[2] I. Doğan, M. C. M. van de Sanden, *Plasma Process. Polym*. **2016**, *13*, 19.

[3] C. Arpagaus, G. Oberbossel, P. R. von Rohr, *Plasma Process. Polym*. **2018**, *15*, 1800133.

[4] K. Ostrikov, U. Cvelbar, B. Murphy, *J. Phys. D: Appl. Phys*. **2011**, *44*, 174001.

[5] L. Boufendi, M. Ch. Jouanny, E. Kovacevic, J. Berndt, M. Mikikian, *J. Phys. D: Appl. Phys*. **2011**, *44*, 174035.

[6] S. C. Wong, J. Goree, Z. Haralson, B. Liu, *Nature Physics* **2018**, *14*, 21.

[7] S. V. Vladimirov, K. Ostrikov, *Phys. Rep*. **2004**, *393,* 175.

[8] V. E. Fortov, A. V. Ivlev, S. A. Khrapak, A. G. Khrapak, G. E. Morfill, *Phys. Rep*. **2005**, *421*, 1.

[9] P. K. Shukla, B. Eliasson, *Rev. Mod. Phys*. **2009**, *81*, 25.

[10] H. Kersten, H. Deutsch, E. Stoffels, W. W. Stoffels, G. M. W. Kroesen, R. Hippler, *Contrib. Plasma Phys*. **2001**, *41*, 598.

[11] S. Hong, J. Berndt, J. Winter, *Plasma Sources Sci. Technol*. **2003**, *12*, 46.

[12] Ch. Deschenaux, A. Affolter, D. Magni, Ch. Hollenstein, P. Fayet, *J. Phys. D: Appl. Phys*. **1999**, *32*, 1876.

[13] J. Benedikt, A. Consoli, M. Schulze, A. von Keudell, *J. Phys. Chem. A* **2007**, *111*, 10453.

[14] H. C. Thejaswini, S. Peglow, U. Martens, V. Sushkov, R. Hippler, *Contrib. Plasma Phys*. **2014**, *54*, 683.

[15] H. T. Do, G. Thieme, M. Frohlich, H. Kersten, R. Hippler, *Contrib. Plasma Phys*. **2005**, *45*, 378.

[16] J. Winter, J. Berndt, S. H. Hong, E. Kovačević, I. Stefanović, O. Stepanović, *Plasma Sources Sci. Technol.* **2009**, *18*, 034010.

[17] A. P. Herrendorf, V. Sushkov, R. Hippler, *J. Appl. Phys*. **2017**, *121*, 123303.

[18] J. Berndt, E. Kovacevic, I. Stefanovic, L. Boufendi, *J. Appl. Phys*. **2009**, *106*, 063309.

[19] I. Stefanović, N. Sadeghi, J. Winter, B. Sikimić, *Plasma Sources Sci. Technol.* **2017**, *26*, 065014.

[20] Th. Wegner, A. M. Hinz, F. Faupel, T. Strunskus, H. Kersten, J. Meichsner, *Appl. Phys. Lett*. **2016**, *108*, 063108. [21] I. B. Denysenko, E. von Wahl, S. Labidi, M. Mikikian, H. Kersten, T. Gibert, E. Kovacevic, N. A. Azarenkov, *Plasma Phys. Control. Fusion* **2019**, *61*, 014014.

[22] S. Stoykov, C. Eggs, U. Kortshagen, *J. Phys. D: Appl. Phys*. **2001**, *34*, 2160.

[23] K. De Bleecker, A. Bogaerts, W. Goedheer, *Phys. Rev. E* **2006**, *73*, 026406.

[24] M. Mao, J. Benedikt, A. Consoli, A. Bogaerts, *J. Phys. D: Appl. Phys*. **2008**, *41*, 225201.

[25] D. A. Ariskin, I. V. Schweigert, A. L. Alexandrov, A. Bogaerts, F. M. Peeters, *J. Appl. Phys.* **2009**, *105*, 063305.

[26] I. V. Schweigert, A. L. Alexandrov, D. A. Ariskin, *Plasma Chem. Plasma Process*. **2014**, *34*, 671.

[27] A. Akhoundi, G. Foroutan, *Phys. Plasmas* **2017**, *24*, 053516.

[28] K. Ostrikov, H.-J. Yoon, A. E. Rider, S. V. Vladimirov, *Plasma Process. Polym*. **2007**, *4*, 27.

[29] A. M. Hinz, E. von Wahl, F. Faupel, T. Strunskus, H. Kersten, *J. Phys. D: Appl. Phys*. **2015**, *48*, 055203.

[30] A. Hurlbatt, A. R. Gibson, S. Schröter, J. Bredin, A. P. S. Foote, P. Grondein, D. O'Connell, T. Gans, *Plasma Process. Polym*. **2017**, *14*, 1600138.

[31] E. G. Thorsteinsson, J. T. Gudmundsson, *Plasma Sources Sci. Technol*. **2009**, *18*, 045001.

[32] M. A. Lieberman, A. J. Lichtenberg, *Principles of Plasma Discharges and Materials Processing* 2nd edn., Wiley, New York **2005**.

[33] J. T. Gudmundsson, *Plasma Sources Sci. Technol.* **2001**, *10*, 76.

[34] V. A. Godyak, R. B. Piejak, B. M. Alexandrovich, *Plasma Sources Sci. Technol*. **1992**, *1*, 36.

[35] I. B. Denysenko, H. Kersten, N. A. Azarenkov, *Phys. Rev. E* **2015**, *92*, 033102.

[36] I. B. Denysenko, H. Kersten, N. A. Azarenkov, *Phys. Plasmas* **2016**, *23*, 053704.

[37] http://webbook.nist.gov

[38] M. Mikikian, L. Boufendi, A. Bouchoule, H. M. Thomas, G. E. Morfill, A. P. Nefedov, V. E. Fortov, The PKE-Nefedov Team, *New J. Phys.* **2003**, *5*, 19.

[39] S. A. Khrapak, S. V. Ratynskaia, A. V. Zobnin, A. D. Usachev, V. V. Yaroshenko, M. H. Thoma, M. Kretschmer, H. Höfner, G. E. Morfill, O. F. Petrov, V. E. Fortov, *Phys. Rev. E* **2005**, *72***,** 016406.

[40] M. Hundt, P. Sadler, I. Levchenko, M. Wolter, H. Kersten, K. Ostrikov, *J. Appl. Phys.* **2011**, *109*, 123305.

[41] F. M. J. H. van de Wetering, S. Nijdam, J. Beckers, *Appl. Phys. Lett*. **2016**, *109*, 043105.

# Graphical Abstract

**Properties of an Ar/C₂H₂ plasma are studied using a volume-averaged model for the process conditions of our experiments on nanoparticle growth.** It is analyzed how the densities of plasma species, initiating the formation of carbonaceous nanoparticles, depend on the input power, the acetylene input flux, the shape of the electron energy distribution function and the density of nanoparticles.

I. B. Denysenko\*, E. von Wahl, S. Labidi, M. Mikikian, H. Kersten, T. Gibert

**Effects of Process Conditions on the Chemistry of an Ar/C₂H₂ Dust-Forming Plasma**